Vaccine xxx (xxxx) xxx

Contents lists available at ScienceDirect

Vaccine

journal homepage: www.elsevier.com/locate/vaccine

An intranasal nanoparticle vaccine elicits protective immunity against *Mycobacterium tuberculosis*

K M Samiur Rahman Sefat [a,1], Monish Kumar [a,1], Stephanie Kehl [b], Rohan Kulkarni [a], Ankita Leekha [a], Melisa-Martinez Paniagua [a], David F. Ackart [c], Nicole Jones [b], Charles Spencer [b], Brendan K Podell [c], Hugues Ouellet [b], Navin Varadarajan [a,*]

[a] Department of Chemical and Biomolecular Engineering, University of Houston, Houston, TX 77054, USA
[b] Department of Biological Sciences, University of Texas, El Paso, TX 79968, USA
[c] Mycobacteria Research Laboratories, Department of Microbiology, Immunology and Pathology, Colorado State University, Fort Collins, CO 80523, USA

ARTICLE INFO

Keywords:
Intranasal vaccine
Adjuvant
Nanoparticles
Tuberculosis

ABSTRACT

Mucosal vaccines have the potential to elicit protective immune responses at the point of entry of respiratory pathogens, thus preventing even the initial seed infection. Unlike licensed injectable vaccines, mucosal vaccines comprising protein subunits are only in development. One of the primary challenges associated with mucosal vaccines has been identifying and characterizing safe yet effective mucosal adjuvants that can effectively prime multi-factorial mucosal immunity. In this study, we tested NanoSTING, a liposomal formulation of the endogenous activator of the stimulator of interferon genes (STING) pathway, cyclic guanosine adenosine monophosphate (cGAMP), as a mucosal adjuvant. We formulated a vaccine based on the H1 antigen (fusion protein of Ag85b and ESAT-6) adjuvanted with NanoSTING. Intranasal immunization of NanoSTING-H1 elicited a strong T-cell response in the lung of vaccinated animals characterized by (a) $CXCR3^{+}$ $KLRG1^{-}$ lung resident T cells that are known to be essential for controlling bacterial infection, (b) IFNγ-secreting $CD4^{+}$ T cells which is necessary for intracellular bactericidal activity, and (c) IL17-secreting $CD4^{+}$ T cells that can confer protective immunity against multiple clinically relevant strains of *Mtb*. Upon challenge with aerosolized *Mycobacterium tuberculosis* Erdman strain, intranasal NanoSTING-H1 provides protection comparable to subcutaneous administration of the live attenuated *Mycobacterium bovis* vaccine strain Bacille–Calmette–Guérin (BCG). Our results indicate that NanoSTING adjuvanted protein vaccines can elicit a multi-factorial immune response that protects from infection by *M. tuberculosis*.

1. Introduction

Due in part to the lack of an efficient vaccine, *Mycobacterium tuberculosis* (*Mtb*) infection remains one of the significant causes of death worldwide [1]. Bacille Calmette-Guérin (BCG), the only vaccine against tuberculosis (TB), has a range of protective efficacy against adult pulmonary TB, ranging from 0 % to 80 % in clinical trials [2]. Being a live attenuated vaccination, BCG is also not advised for those with weakened immune systems, including newborns with HIV [3]. The development of vaccines that can either supplement or replace BCG to provide a protective immune response against pulmonary TB has received much attention. One advantage of subunit vaccinations is that they typically have better safety profiles than live attenuated vaccines, which cannot always be administered to immunocompromised individuals. An adjuvant is necessary to elicit a robust memory immune response to the antigen in subunit vaccines. However, there is a lack of authorized adjuvants that can safely induce antigen-specific effector and memory $CD4^{+}$ and $CD8^{+}$ T cells [4,5].

It is well acknowledged that the mucosal immune response is essential for preventing respiratory infections such as TB [6]. Dendritic cells (DCs), which transport the vaccinated antigen to local and systemic inductive sites such as the lymph nodes and spleen, cause both mucosal and systemic reactions due to mucosal vaccination [7,8]. The widespread use of several effective mucosal vaccinations against non-respiratory pathogens such as polio, cholera, rotavirus, and salmonella [9] has demonstrated the viability and safety of this strategy.

* Corresponding author at: Department of Chemical and Biomolecular Engineering, University of Houston Houston, Texas, TX 77204, USA.
E-mail address: nvaradar@central.uh.edu (N. Varadarajan).
[1] These authors have contributed equally to this work.

https://doi.org/10.1016/j.vaccine.2024.04.055
Received 19 October 2023; Received in revised form 15 April 2024; Accepted 18 April 2024

The cyclic dinucleotide, 2′-3′ cyclic GMP–AMP (cGAMP), has emerged recently as a potent adjuvant that can be co-delivered with subunit proteins and is effective in enhancing humoral, cellular, and mucosal immune responses [10]. cGAMP binds to the stimulator of interferon genes (STING), leading to the oligomerization of STING and its translocation to the *trans*-Golgi network, initiating a signaling cascade that culminates in the secretion of type I and type III interferons [11]. Due to its immunostimulatory role, cGAMP is being investigated as an immunotherapeutic for treating cancers and a mucosal adjuvant for developing vaccines against infectious diseases [12]. STING activating cyclic dinucleotide adjuvant used in a mucosal protein subunit vaccine against TB elicited both Th1 and Th17 immune responses in mice [5]. An ESAT-6-based c-di-AMP adjuvanted mucosal vaccine decreased bacterial load in the lungs of challenged animals [13]. When taken as a whole, these data offer a strong case for using STING agonists as a clinical TB vaccine adjuvant.

In this manuscript, we tested the efficacy of NanoSTING, a liposomal formulation of cGAMP, as a mucosal adjuvant against TB. Previously, we had shown that the adjuvant provides multi-faceted protection against major SARS-CoV-2 variants in circulation [14,15]. We anticipate that the liposomal formulation offers two advantages. First, since 2′3′-cGAMP is rapidly degraded by ENPP-1 and has a half-life of ~ 30 min *in vivo* [16], encapsulation inside nanoparticles can lead to improved half-life and bioavailability [17]. Second, as we have previously demonstrated, liposomal nanoparticles facilitate the decoration of multiple copies of the protein antigen on the liposomal surface, leading to enhanced immunogenicity [18]. Here, we found that intranasal administration of a fusion protein (H1 antigen) comprised of Ag85b and ESAT-6 adjuvanted with NanoSTING conferred protection against virulent *Mtb*. The protection provided by the vaccine was comparable to the subcutaneous vaccination with BCG. We also observed a surge of T-cell response induced by the adjuvant in the lung and spleen of immunized animals. Post-vaccination monitoring of the animal body weights over six weeks indicated that the vaccine was well tolerated in mice. This study suggests that NanoSTING is a potent mucosal adjuvant against *Mtb* that warrants further investigation with next-generation TB antigens, which might yield even better protection than the current formulation.

2. Materials and methods

2.1. Plasmid design

The protein sequence encoding *Mtb-secreted* antigen Ag85b (Accession Code: AY207396.1) and ESAT-6 (Accession code: AF226277.1) were downloaded from Genbank. The H1 antigen gene block was created at IDT (Coralville, Iowa), and we optimized the codons for expression in *Escherichia coli*. We used Gibson Assembly to insert the gene block sequence, which included the Sumo tag and the full-length H1 antigen gene, under the control of a T7 promoter in the plasmid backbone of the pET28A(+) plasmid after cutting it at the NdeI and XhoI restriction sites. Electroporation on electrocompetent *E. coli* EC10 cells was used for bacterial transformation and plasmid propagation.

2.2. Protein expression and purification

Briefly, *E. coli* BL21(DE3) cells were transformed with the plasmid encoding recombinant Sumo-H1 Ag protein. Cells were seeded in 500 mL of Luria-Bertani broth and cultured at 37 °C until the OD_{600} reached 0.6. The next step was stimulating Sumo-H1 Ag expression using 1 mM IPTG for 5 h. Cells were harvested and suspended in 20 mL buffer A (100 mM NaH_2PO_4, 10 mM Tris-Cl, 8 M Urea [pH 8]) and lysed by sonication: four cycles (each at 10 s on at 30 % amplitude, 20 s off, at 4 °C). Urea in buffer A solubilized the inclusion bodies. The lysate was then centrifuged at 20,000*g* for 30 min at 4 °C to remove cell debris and subjected to immobilized metal affinity chromatography (IMAC).

For IMAC purification, the lysate was loaded onto a gravity flow column with Ni-Sepharose High-Performance resin, which had been previously equilibrated for 20 min with 20 mL Buffer A. The column was then washed with 10 CV of Buffer B (100 mM NaH_2PO_4, 10 mM Tris-Cl, 8 M Urea [pH 6.3]), and the bound proteins were eluted with Buffer C (100 mM NaH_2PO_4, 10 mM Tris-Cl, 8 M Urea [pH = 5.9]).

The eluted protein was dialyzed against Factor Xa digestion buffer (20 mM Tris, 50 mM NaCl, 100 mM Urea, 1 mM $CaCl_2$, pH = 8.0) and then incubated with Factor Xa overnight at 4 °C to remove the Sumo tag. The cleaved protein was then dialyzed against sterile PBS to precipitate the H1 antigen selectively while the Sumo tag remained soluble. The subsequent steps were performed using sterile reagents and endotoxin-free labware to keep endotoxin to a minimum. The precipitated protein was then centrifuged at 10,000*g* for 10 min to form a pellet, and the pellet was redissolved in 8 M urea solution to solubilize the protein. Finally, the soluble protein was dialyzed against 50 mM L-Arg, 50 mM L-Glu, 50 mM Na_2HPO_4, 0.05 % Tween-20, pH = 8.5, and stored at −20 °C until further use. We tested the endotoxin level in the final protein solution using Pierce™ LAL Chromogenic Endotoxin Quantitation Kit (ThermoFisher Scientific, MA, USA) and confirmed that the total amount of endotoxin delivered intranasally was < 5 EU per mouse.

2.3. Preparation of NanoSTING and vaccine formulation

Preparation and characterization of cGAMP encapsulation liposomes were described previously [14]. Briefly, the liposomes were synthesized with a molar ratio of 10:1:1:1 for DPPC, DPPG, Cholesterol (Chol), and DPPE-PEG2000. We combined the lipids with $CHCl_3$ and CH_3OH to create the liposomes. Then, we evaporated the mixture using a vacuum rotary evaporator for around 80 min at 45 °C. We dried the resulting lipid thin film until all organic solvents evaporated. We added a pre-warmed cGAMP solution (0.3 mg/mL in PBS buffer at pH 7.4) to hydrate the lipid film. The hydrated lipid films were mixed at 65 °C and subjected to freeze–thaw cycles. We sonicated the mixture with a Branson Sonicator for 60 min (40 kHz). The free untrapped cGAMP was removed by Amicon Ultrafiltration units (MW cut off 10 kDa). We used PBS buffer to wash the cGAMP-liposomes three times thoroughly. Using a calibration curve for cGAMP at 260 nm, the Take3 Micro-Volume absorbance analyzer of Cytation 5 (BioTek) was used to determine the amount of cGAMP in the filtrates. By deducting the quantity of free cGAMP in the filtrate, we determined the final concentration of liposomal-encapsulated cGAMP and encapsulation efficiency.

We mixed H1 antigen with the NanoSTING suspensions at room temperature for 10 min to allow the protein to adsorb onto the liposomes. The formulated vaccine was stored at 4 °C and used for up to two months. We stored the NanoSTING suspensions at 4 °C, and they were stable for 11 months [14]. The average particle diameter, polydispersity index, and zeta potential were characterized at room temperature by the Litesizer 500 (Anton Paar).

2.4. Bacterial strains and culture

Mtb Erdman and *M. bovis* BCG were obtained from Dr. Jeffery S. Cox (University of California at Berkeley). Mycobacteria were cultivated at 37 °C in 1 L roller bottles containing 100 mL of Middlebrook 7H9 (Difco) broth supplemented with 10 % (*v/v*) Oleic-Albumin-Dextrose-Catalase (OADC), 0.2 % (*v/v*) glycerol, and 0.05 % (*v/v*) Tween-80. For quantification of colony-forming-units (CFUs), bacterial suspension and tissue homogenates were spread onto solid Middlebrook 7H10 agar medium supplemented with 10 % (*v/v*) OADC, 0.5 % (*v/v*) glycerol, and 100 μg/mL cycloheximide. Mycobacteria were grown at 37 °C for 3–4 weeks.

2.5. Mice immunization and Mtb challenge

All animal experiments complied with the Institutional Animal Care and Use Committee (IACUC) of the University of Houston and the University of Texas at El Paso (UTEP). For the immunogenicity study,

groups of six- to ten-week-old female C57BL/6 mice were purchased from The Jackson Laboratory (ME, USA) and adapted in the UH animal facility for 10 days before the start of the experiment. The animals were immunized intranasally with groups: 1) PBS, 2) 10 μg H1 antigen, and 3) 10 μg H1 antigen + 20 μg NanoSTING. For all the groups, we administered 20–25 μL of the appropriate formulation. Four weeks after the initial immunization, the animals were boosted with the corresponding first dosage. Six weeks from the day of the first dosage, the animals were euthanized, and lung and spleen samples were collected for ELISPOT and ICS assays.

Groups of five-week-old female C57BL/6 mice were obtained from The Jackson Laboratory and were acclimated in the UTEP ABSL-2 vivarium for one week before immunization. Six weeks before the challenge, two groups of mice (n = 26) were anesthetized by isoflurane inhalation for three minutes. Then, either the vaccine formulation or PBS alone as an unvaccinated control was applied to the nares for inhalation. At two weeks pre-challenge, mice received a booster as described above. As a positive control, one group of mice (n = 26) was injected subcutaneously once with approximately 5×10^5 CFU of *M. bovis* BCG in a volume of 200 μl of PBS at six weeks pre-challenge. One week before the *Mtb* challenge, all the mice were moved to an ABSL-3 room for acclimation. We aerosolized an *Mtb* suspension at OD_{600} of 0.2 on day 0 to infect the mice. We sacrificed six animals on day 1 and determined the average bacterial burden to be 500 CFU [19]. The health of the animals was monitored daily, and body weight was measured weekly.

2.6. Organ processing post-challenge CFU

At 3- and 10 weeks post-exposure, groups of mice (n = 4–5) were sacrificed for CFU determination in lung, spleen, and liver homogenates and histological analyses. For CFU determination, organs were homogenized in gentleMACS C tubes (Miltenyi Biotec) with 2 mL of PBS. Serial dilutions of the homogenates were spread onto 7H10-OADC agar media containing 100 μg/mL cycloheximide, and plates were incubated at 37 °C for at least three weeks. For histology, the lungs were inflated through the trachea with 2–3 mL of 10 % neutral-buffered formalin (NBF) before dissection. Organs were stored at 4 °C in 10 % NBF. For antigen recall and flow cytometry analyses, a group of mice (n = 5) were euthanized at 4- and 10 weeks post *Mtb* exposure. Lung and spleen tissues were collected, diced, and homogenized in gentleMACS C tubes, following Milteny Biotec's protocols for Mouse Lung and Spleen Dissociation, respectively. Erythrocytes were removed by washing the cell pellets with 1X Red Blood Cell Lysis buffer (Miltenyi Biotec). Cells were enumerated with Trypan Blue (0.04 %) exclusion using a hemocytometer. Washed cells were resuspended at a density of 1–2.0 x 10^7 cells/mL in RPMI 1640 (Corning) containing 10 % fetal bovine serum (FBS) (Corning) (R10) and freshly supplemented with 50 μM 2-mercaptoethanol (Sigma Aldrich) and 1 % (*w/v*) penicillin–streptomycin (Gibco). We stored the unused cells in a liquid Nitrogen storage tank, suspended in a freezing medium containing 90 % FBS and 10 % DMSO until further use.

2.7. Processing of spleen and lungs for ELISPOT

We utilized 5 mL of 0.1 mM EDTA in PBS without Ca^{2+} or Mg^{2+} to perfuse the lung vasculature and injected it into the right cardiac ventricle to isolate lung cells. Each lung was divided into 100–300 mm^2 pieces with a knife. We transferred the minced lung tissue in a digestion buffer containing collagenase D (2 mg/mL, Roche) and DNase (0.125 mg/mL, Sigma) in 5 mL of RPMI. The tissue was incubated in the digestion buffer at 37 °C for 1 h and 30 min while vortexing every 10 min. We disrupted the remaining intact tissue by passage (6–8 times) through a 21-gauge needle. The reaction was then put on hold by adding 500 μL of an ice-cold reaction-stopping buffer (1x PBS, 0.1 M EDTA). Next, we passed the suspension through a 40 μm disposable cell strainer (Falcon) to remove large tissue pieces and collected the single cells in a 50 mL tube. The cells were centrifuged at 600 x *g* for 10 min to form a pellet. The red blood cells (RBCs) were subsequently lysed by resuspending the cell pellet in 3 mL of ACK Lysing Buffer (Invitrogen), then centrifuged again at 600 x *g* for 10 min. After the supernatants were discarded, the cell pellets were resuspended in 5 mL of full RPMI media (Corning). Next, we stored the spleens in RPMI medium until they were ready for processing. Spleens were homogenized by pushing them through a 40 μm cell strainer using the hard end of a syringe plunger. Then, we removed RBCs from splenocytes by incubating them in 3 mL of ACK lysis solution for 3 min at room temperature. Finally, we passed the mixture through a 40 μm strainer to get a single-cell suspension. We used the trypan blue exclusion method to count the number of splenocytes and lung cells.

2.8. ELISPOT

We used the Mouse IFNγ ELISPOT Basic Kit (ALP) to perform the IFNγ ELISPOT according to the manufacturer's instructions (Mabtech, VA, USA). We incubated the ELISPOT plates (Ref: MSIPS4W10, Millipore) with AN18 IFNγ (1 μg/mL, Mabtech #3321-3-250;) overnight coating antibody at 4 °C. The plates were washed five times with sterile PBS before adding lung lymphocytes or splenocytes. Fresh cells from each animal were treated in four different groups: 1) negative control (R10 medium), 2) positive control (10 ng/mL phorbol 12-myristate 13-acetate (PMA) (Sigma, St. Louis, MI, USA) and 1 μg/mL of ionomycin), 3) Ag85b peptide pool (1.4 μg/mL/peptide, JPT, Germany) and 4) ESAT-6 peptide pool (2 μg/mL/peptide, BEI Resources, VA, USA). Lung lymphocytes and splenocytes were added to the plate in triplicates, where 3×10^5 cells were added for negative controls, Ag85b, and ESAT-6 peptide pool stimulation. For positive control stimulation, we only added 1×10^4 cells. The cells were stimulated for 16 h. We washed off the cells the following day and incubated the plates with a biotinylated R4-6A2 anti-IFNγ- (Mabtech #3321-6-250) detection antibody. Following the wash, we treated the wells for 1 h at room temperature with diluted Extravidin-ALP conjugate (1:30,000). (Sigma, St. Louis, MI, USA). Then, we added 70 μL/well of BCIP/NBT-plus substrate (Mabtech #3650-10) to the plate to produce the spots. Finally, the substrate was rinsed off with water after 20–30 min incubation. The spots were measured using Cytation 7 (BioTek Instruments, Inc.). Every spot represents a different cytokine-secreting cell. We displayed the values as the average of measured triplicates with the background eliminated.

2.9. Post-challenge intracellular cytokine staining

Antigen recall, staining, and flow cytometry analysis determined ESAT-6 and Ag85b-specific lung and spleen T-cell responses. We used the cryopreserved lung and spleen cells for these experiments. Briefly, In 96-well round-bottom plates, cells ($1–2 \times 10^6$ lung or spleen cells/well) were aliquoted and stimulated at 37 °C, 5 % CO_2 for 12 h with 1.4 μg/mL of Ag85b and 2 μg/mL ESAT-6 peptides. As positive and negative controls, cells were incubated with PMA (10 ng/mL), ionomycin (1 μg/mL), or media alone. To allow cytokine accumulation, 50 μL of GolgiStop (BD Biosciences) diluted 1:500 in R10 medium was added to each well and further incubated at 37 °C, 5 % CO^2 for 4 h. Cells were pelleted by centrifugation at 300 × *g* for 5 min, and supernatants were collected and kept frozen at −80 °C for cytokine profiling.

For labeling, cells were washed with PBS and then incubated with Live/Dead Zombie Green (Biolegend; cat. no 423112). Fc receptors were blocked with unlabeled anti-mouse CD16/CD32 (clone 2.4G2; BD Biosciences). After washing with FACS buffer (PBS + 2 % FBS), cell surface markers were stained with anti-mouse CD3- PerCPCy5.5 (Biolegend; cat. no 100218), CD4- PE-Cy7 (Biolegend; #100422), CD8-Spark Blue 574 (Biolegend; cat. no 100794), KLRG1-BV510 (Biolegend; cat. no 138421), and CXCR3- Alexa Fluor 700 (Biolegend; cat. no 353742). We fixed the cells with BD CytoFix/Perm and washed them thoroughly with BD Perm/Wash solution. Intracellular cytokines were labeled with anti-

mouse IFNγ-APC (Biolegend; cat. no 505810) and IL17-Pacific Blue (Biolegend; cat. no 506918) prepared in BD Perm/Wash solution, and then the cells were washed with Perm/Wash buffer. Cells were stained with the Live-Dead Zombie Green for compensation controls and labeled with the same panel of antibodies, individually or in FMO combinations. Samples were finally transferred into 5-mL polystyrene round-bottom test tubes with a cell strainer snap cap (Corning). Data was acquired on a BD LSRFortessa X-20 flow cytometer apparatus and analyzed using FlowJo™ v10.8 Software (BD Life Sciences).

2.10. Biodistribution studies

We used fluorescently labeled H1 antigen as a distribution marker to observe the effect of liposomal adjuvants on the residence time of the protein antigen. The iFluor 647 maleimide dye (AAT Bioquest, Pleasanton, CA) was conjugated to H1 antigen according to the manufacturer-recommended protocol. Next, we intranasally administered 25 μL of a mixture of H1 antigen-iFluor 647 and NanoSTING (12.5 μL in each nostril) into BALB/c mice. The biodistribution of the dye was visualized at different time points after immunization using an *in vivo* imaging system (PerkinElmer, Waltham, MA). The fluorescence strength was quantified within regions of interest using the ImageJ (Easter Greenbush, NY) image processing program.

2.11. ELISA

We tested the magnitude of vaccine-induced antibody response in serum against Ag85b using ELISA. In short, we incubated high protein binding ELISA plates (Corning, NY, USA) with Ag85b protein (Abcam, MA, USA) at 0.25 μg/mL in phosphate-buffered saline (PBS) overnight at 4 °C or for 2 h at 37 °C. We washed the plates with PBS + 0.05 % Tween20 (PBST) to remove unbound protein. The plates were blocked with PBS + 1 % BSA (Fisher Scientific, PA, USA) + 0.1 % Tween20 for 2 h at room temperature. Following three more washes with PBST, we added the serum samples at different dilutions to the plate. We washed the plates with PBST and added HRP-conjugated anti-mouse IgG (Jackson ImmunoResearch Laboratories, 1:20000; PA, USA). Finally, we developed the plates using 1-Step™ TMB ELISA substrate (ThermoFisher Scientific).

2.12. Histopathology

Lungs fixed in 10 % neutral buffered formalin were processed and embedded in paraffin blocks, cut as 5 μm sections, and slides stained with hematoxylin and eosin using routine histology methods. Slides were scanned on a Vectra Polaris scanning microscope (Akoya Biosciences, Marlborough, MA) using the brightfield setting at 20× magnification. These digital images were analyzed using Visiopharm image analysis software (Visiopharm, Westminster, CO), employing a custom designed algorithm for the detection of tuberculosis pathology in lung tissue. Briefly, for each tissue section, a region of interest (ROI) identification algorithm was generated at a low magnification with custom decision forest training and classification to differentiate tissue versus background based on color and area. Tissue lesions were identified within tissue ROIs using a formulated K-means clustering algorithm based on staining intensity, area, and morphological features of inflammation. Lesion burden was expressed as a percent ratio between area of TB lesion pathology and total lung tissue area.

2.13. Statistical analysis

All data are presented as mean values, and error bars represent SEM. We performed all statistical analyses using GraphPad Prism (v8). We used the Mann-Whitney *t*-test for pairwise comparisons. To compare multiple groups, we used Dunn's multiple comparison test. We performed Tukey's multiple test for repeated measures analysis to compare bodyweight and bacterial load data at each time point.

3. Results

3.1. H1 Antigen Protein expression and vaccine formulation

H1 is a synthetic fusion protein comprising two different *Mtb* antigens and has been tested in humans [20,21]. Despite our initial attempts to make soluble protein in *E. coli*, we were unsuccessful (data not shown). To enhance the solubility and expression of the H1 antigen, we fused a Sumo-tag to the N terminus of the protein with a Factor Xa cleavage site between them (Fig. 1**A**). The protein was purified using standard Ni^{2+}-NTA chromatography and the Sumo-tag was removed by factor Xa proteolysis (Supplementary Fig. 1). Unfortunately, upon proteolysis, the H1 antigen rapidly precipitated out of solution. To ensure that we have soluble protein for immunization, we resolubilized the protein using 8 M urea, followed by dialysis of the resulting protein in a buffer containing known protein stabilizers (50 mM L-Arg and 50 mM L-Glu) (Supplementary Fig. 1) [22]. Our expression system using the Sumo-tag yielded ~40 mg/L of purified protein (Fig. 1**B**).

We used the single-step "mix and immunize" approach to prepare the final vaccine formulation NanoSTING-H1, as described previously [14]. As H1 antigen aggregates rapidly in PBS, we wanted to test if the NanoSTING-H1 formulation was stable for intranasal vaccination. We utilized dynamic light scattering (DLS) to compare particle sizes of the nanoparticle adjuvant and protein mixture. Both NanoSTING and NanoSTING-H1 showed similar particle sizes, 118 ± 1.6 nm (mean ± SEM) and 130 ± 1.8 nm, respectively, indicating no rapid protein aggregation in our vaccine formulation, at least during short-term incubation (30 min – 1 h) at 25 °C (Fig. 1**C**).

3.2. Intranasal immunization with NanoSTING increases the retention time of the immunogen in the nasal cavity

In addition to stabilizing the protein and increasing the avidity of display, liposomal formulations can increase the antigen's residence time within the mucosal compartment, facilitating a robust immune response [23,24]. Typical protein antigens administered intranasally have a short residence time in the nasal cavity and are cleared in less than 1 h [25,26]. We, therefore, wanted to test whether our liposomal adjuvant formulation can delay antigen clearance from the immunization site. To track the antigen *in vivo*, we conjugated the purified H1 antigen with iFluor 647 (Supplementary Fig. 2). We administered H1 iFluor 647 to groups of BALB/c mice, both with or without NanoSTING as an adjuvant and imaged the animals for 24 h using an IVIS Spectrum system. We tracked the antigen by quantifying the total fluorescence signal in a defined region of interest, capturing the mouse nasal cavity (Fig. 2**A**). Longitudinal profiling of the fluorescent H1 antigen in the nasal area of live animals revealed that while the unadjuvanted H1 iFluor 647 was cleared in <4 h, the NanoSTING adjuvanted H1 iFluor 647 was detectable up to 24 h (Fig. 2 **B-D**). We did not observe a fluorescent signal in the lung, but we note that the autofluorescence of the lung is also high, as noted in previous reports [27]. These data suggest that the NanoSTING adjuvanted vaccine has a high residence time in the nasal cavity, thus promoting the likelihood of efficient antigen uptake and processing.

3.3. Intranasal vaccination of mice with NanoSTING-H1 induces cellular immunity in the lung and spleen

To evaluate the immunogenic potential of our experimental vaccine, groups of C57BL/6 mice were vaccinated following a prime/boost vaccination regimen, receiving two doses of (1) NanoSTING-H1, (2) H1 only, and (3) PBS four weeks apart (Fig. 3**A**). The animals were euthanized two weeks after the booster dose, and lung and spleen samples were harvested and processed to isolate single cells. Enzyme-linked

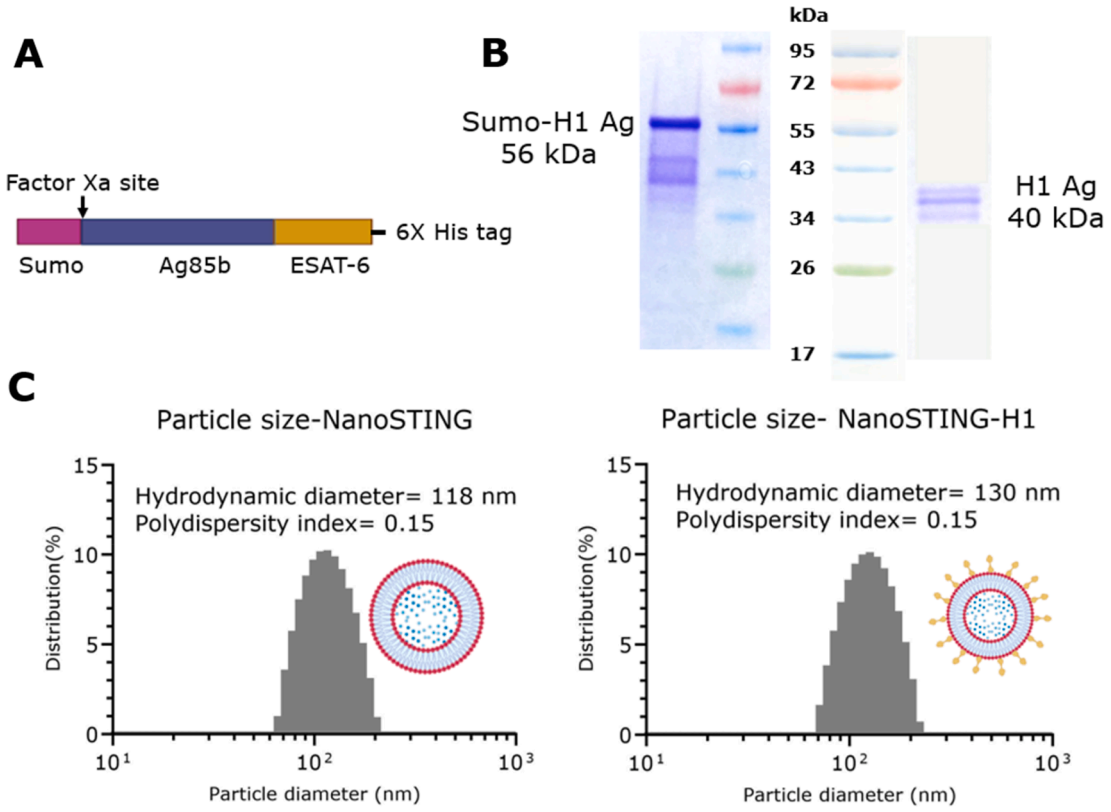

Fig. 1. Design and purification of H1 antigen (Ag85b-ESAT-6) in *E. coli*. A) Construct design for H1 antigen with a cleavable Sumo-tag for enhanced protein expression and solubility. **B)** SDS-page of the purified Sumo-H1 protein (56 kDa) and purified soluble H1 antigen (40 kDa). **C)** Physical characterization of NanoSTING, NanoSTING-H1 by DLS.

immunospot (ELISPOT) assay was performed using the lung and spleen cells to determine if NanoSTING-H1 elicits Th1 immunity, as Th1 cytokine-secreting T cells are essential for the control of *Mtb* infection [28]. NanoSTING-H1 induced antigen-specific IFNγ-secreting T cells in the lungs of vaccinated animals (Ag85b: 670 ± 127 SFC/10^6 cells, ESAT-6: 98 ± 30 SFC/10^6 cells), which was significantly higher when compared to H1 (Ag85b: 16 ± 5 SFC/10^6 cells, p-value < 0.001; ESAT-6: 3 ± 2, SFC/10^6cells, p-value < 0.0001) and unvaccinated groups (Ag85b: 9 ± 5 SFC/10^6 cells, p-value = 0.005; ESAT-6: 6 ± 1 SFC/10^6 cells, p-value = 0.004) (Fig. 3**B**). Similarly in spleen, vaccination with NanoSTING-H1 resulted in significantly higher antigen-specific T cells (Ag85b: 520 ± 63 SFC/10^6 cells, ESAT-6: 90 ± 23 SFC/10^6 cells) compared to H1 (Ag85b: 39 ± 11 SFC/10^6 cells, p-value < 0.001; ESAT-6: 5 ± 3 SFC/10^6cells, p-value < 0.001) and unvaccinated (Ag85b: 13 ± 5 SFC/10^6 cells, p-value = 0.0014; ESAT-6: 5 ± 2 SFC/10^6cells, p-value = 0.0097) groups (Fig. 3**C**).

Besides Th1 responses, it has been previously demonstrated that a higher frequency of IL-17 secreting $CD4^+$ T cells (Th17) in the lung can confer robust protection against virulent *Mtb* [29]. To quantify the Th17 responses in the lung, we performed intracellular cytokine staining (ICS) and flow cytometry (Supplementary Fig. 3). These data reveal that intranasal vaccination with NanoSTING-H1 induced significantly higher IL-17 secreting $CD4^+$ T cells (0.78 % ± 0.16 %) in the lung when compared to the other two groups of animals (0.43 % ± 0.26 % for H1, and 0.07 ± 0.04 % for unvaccinated animals, p-value = 0.03) (Fig. 3**D**).

Sakai *et al.* have identified a $CXCR3^+KLRG1^-$ lung parenchyma homing T cell population that shows an improved ability to control lung *Mtb* infection [30]. Using flow cytometry, we confirmed that vaccination with NanoSTING-H1 resulted in 5.3 % ± 0.9 % $CXCR3^+$ $KLRG1^-$ parenchymal $CD4^+$ T cells in the lung, which was significantly higher than protein-only (H1) group (1.84 % ± 0.42 %, p-value = 0.015) (Fig. 3**E, F**). Additionally, antigen-specific antibodies may enhance protection against pulmonary TB [31]. Vaccination with NanoSTING-H1 induced Ag85b specific IgG in serum (mean endpoint titers, NanoSTING-H1: 750 ± 350, unvaccinated: 50) that increased after the booster dose (mean endpoint titers, NanoSTING-H1: 3800 ± 3000, unvaccinated: 50) (Supplementary Fig. 5). In summary, NanoSTING-H1 induces Th1-specific cellular immunity, IL-17^+ and $CXCR3^+KLRG1^-$ $CD4^+$ T cells in the lung, and, antigen-specific humoral immunity that may have a synergistic effect in protection against pulmonary TB.

3.4. *NanoSTING-H1 vaccination protects mice against challenge with virulent Mtb strain*

Next, we wanted to determine if our experimental vaccine was protective against live *Mtb* infection. Groups of C57BL/6 mice were vaccinated intranasally with the same prime-boost regimen (Fig. 4**A**). The vaccinated animals were subsequently challenged with aerosolized *M. tb* Erdman. We also vaccinated 10 animals with a single dose of subcutaneous BCG vaccine six weeks before the challenge as a comparative positive control (Fig. 4**A**). As expected, unvaccinated mice showed a significantly higher bacterial burden in the lung (1.30 ± 0.3 × 10^8 CFU, p-value < 0.0001) compared to either the NanoSTING-H1 (1.6 ± 0.2 × 10^6 CFU) or BCG (5.3 ± 0.6 × 10^5 CFU) vaccinated animals (Fig. 4**B**). NanoSTING-H1 and BCG vaccination also limits bacterial replication in the liver and spleen over at least four weeks (**Supplementary Fig. 6**). The reduced bacterial burden in mice corresponds to significantly reduced mean peak weight loss in the NanoSTING-H1 group (1.4 ± 0.5 %), compared to unvaccinated animals (mean peak weight loss of 15.3 ± 1.7 %) (Fig. 4**C**). Finally, we studied the Th1 T cell response in lung following *Mtb* challenge. Consistent with the expectation that vaccination-induced immunity reduces the bacterial burden and could lower the T-cell responses during immediate challenge [5,32], both vaccinated groups BCG (Ag85b: 1.0 ± 0.2 %, ESAT-6: 1.7 ± 0.4 %)

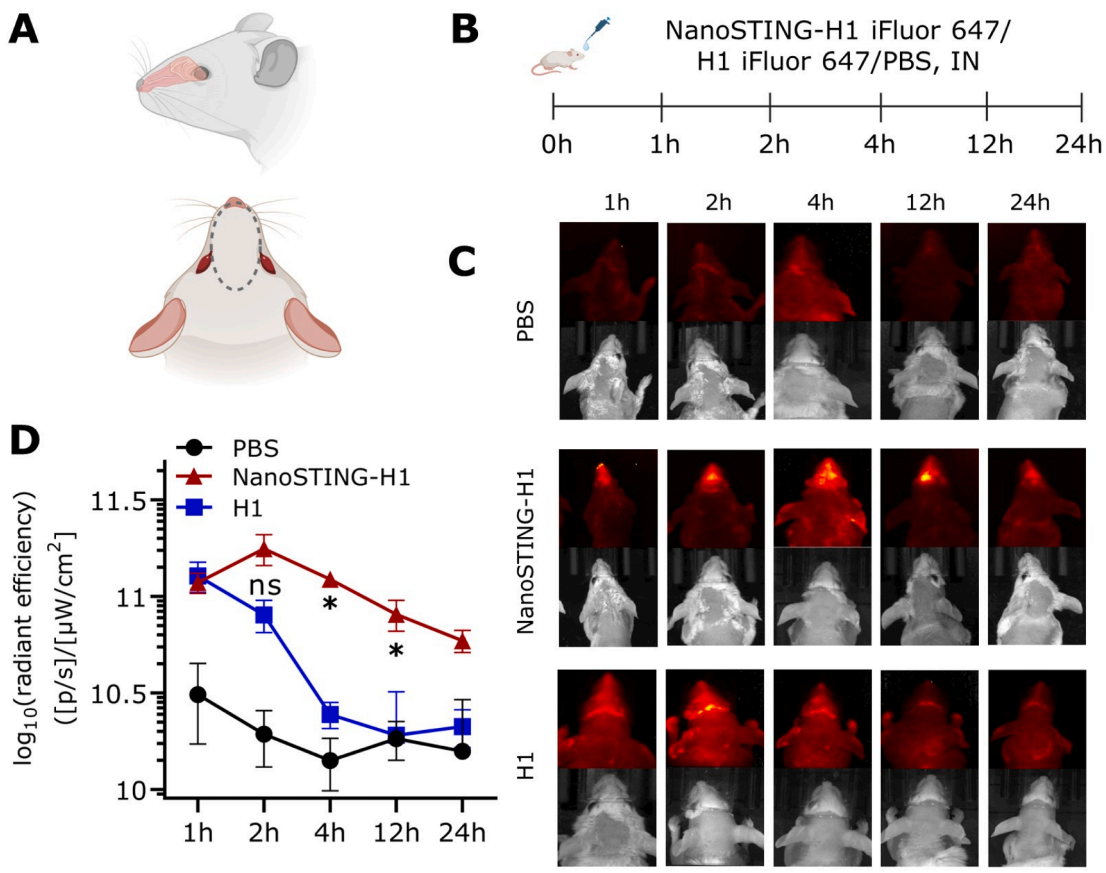

Fig. 2. NanoSTING increases the persistence time of H1 antigen in the nasal cavity of vaccinated animals. A) Mouse schematics illustrating the nasal cavity (top) and the dorsal view of the mouse upper palate (bottom), including the region of interest (ROI) used to quantify fluorescent signals from IVIS images in C and D. **B)** Experimental schema. Mice were inoculated intranasally (IN) with NanoSTING-H1 iFluor 647 (20 µg NanoSTING and 10 µg H1 antigen), H1 Ag iFluor 647 (10 µg) or PBS. Biodistribution was visualized as a factor of light emission from iFluor 647 conjugated protein at different time points. **C)** Representative IVIS images show fluorescence emitted by H1 antigen iFluor 647 in the nasal cavity of BALB/c mice (n = 3/4 animals per group) administered with different vaccine formulations. **D)** Quantified IVIS signals in the nasal cavity over 24 h reported as radiant efficiency (p = photon). The signal calculated from nasal cavity ROI was background corrected by subtracting the signal from nasal-cavity-distal ROI for each mouse. Mann-Whitney *t*-test p values; ns = $p > 0.05$, *$p < 0.05$.

and NanoSTING-H1 (Ag85b: 1.8 ± 0.5 %, ESAT-6: 1.8 ± 0.3 %) did not enhance the frequency of $CD4^+IFN\gamma^+$ T cells beyond the infection-induced (Ag85b: 4.0 ± 0.6 %, ESAT-6: 2.4 ± 0.2 %, *p*-value = 0.0045) values (Fig. 4**D**). A similar observation was also true for the $CD8^+$ T cells; ICS on the lung cells revealed similar frequencies of antigen-specific $CD8^+$ T cells in the lungs of BCG (Ag85b: 0.8 ± 0.2 %, ESAT-6: 0.9 ± 0.2 %) and NanoSTING-H1 (Ag85b: 1.4 ± 0.6 %, ESAT-6: 1.5 ± 0.7 %) vaccinated animals. Both were significantly lower than infection-induced (Ag85b: 3.7 ± 1 %, ESAT-6: 2 ± 0.3 %) levels (Fig. 4**E**).

Lastly, we evaluated the lung immunopathology three- and 10-weeks post-challenge to detect areas of inflammatory lesions on hematoxylin and eosin (H&E) stained tissue sections from the accessory lung lobes. Both BCG and NanoSTING-H1 groups had significantly lower mean lung lesion areas at three (mean lesion percentage: BCG: 9.7 ± 0.6 % and NanoSTING-H1: 13.4 ± 0.7 %) and 10 weeks (BCG: 17.7 ± 0.4 % and NanoSTING-H1: 14.1 ± 0.9 %) after challenge, quantified as the percentage of lesions, compared to the unvaccinated control group (3 weeks post-challenge: 25 ± 4.5 %, *p*-value = 0.0493; 10 weeks post-challenge: 46 ± 5.3 %, *p*-value = 0.0021) (Fig. 5, **Supplementary Fig. 7**). Therefore, intranasal administration of NanoSTING-H1 induces robust immunity in vaccinated animals and protects *Mtb* challenged animals from severe weight loss and inflammatory tissue damage by reducing bacterial burden in lung and other vital organs.

4. Discussion

New and efficient immunization strategies are required due to the BCG's limitations in protecting adults and immunocompromised individuals against pulmonary TB. Owing to considerable safety concerns posed by live-attenuated vaccines, early alternative attempts at an improved TB vaccine included killed bacilli [33,34], and mycobacteria cell extract [34] vaccines. However, instead of providing long-term protection, these vaccines showed an inclination towards inducing a 'hypersensitive' non-specific inflammatory response [35]. Another approach towards a safe and potent TB vaccine is considered secretory or total cell culture protein (CFP)-based vaccines. Despite showing noticeable protective efficacy in animal models [36,37,38], these vaccines present a complex repertoire of protein antigens, which subsequently leads to suboptimal immune response due to competition for antigen presentation [39]. Subunit vaccines can be tailored to recognize key *Mtb* antigens, offering greater control over the specificity of the immune response. As the immunogens used in subunit vaccines are purified and non-essential elements are excluded, these vaccines pose a much lower risk of unwanted inflammatory responses. Several subunit vaccines have been tested in animal models with attractive safety profiles, and currently, a few of them are in clinical trials: M72/AS01E [40], ID93+GLA-SE [41], H56/IC31 [42], and GamTBvac [43]. The principal route of administration for all TB vaccines currently in trials is via injection intramuscularly or intradermally. However, as the lung is where *Mtb* infection first manifests, administering a TB vaccine intranasally can

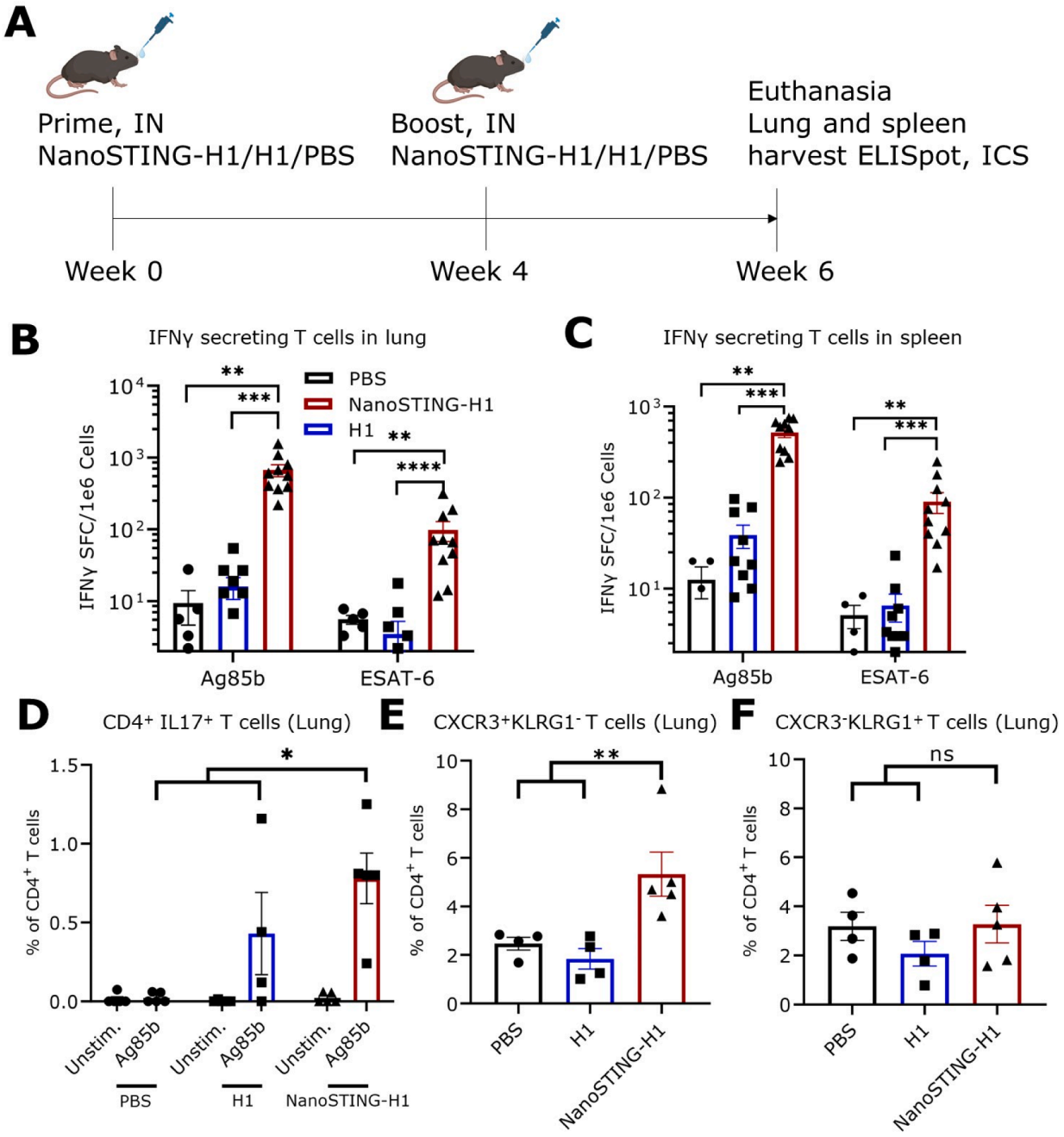

Fig. 3. Intranasal administration of NanoSTING-H1 induces robust T-cell response against multiple antigens in the lung and spleen of vaccinated animals. **A)** The intranasal vaccine was formulated by incubating the purified recombinant protein and adjuvant. We immunized three groups (n = 5–10/group) of animals with intranasally NanoSTING-H1, H1 Ag, and PBS vaccine formulations. Four weeks after the first dose, the animals received an intranasal booster. **B, C)** IFNγ ELISPOT from lung and spleen cells re-stimulated *ex vivo* with Ag85B and ESAT-6 peptide pools seven days after the second boost. Data are expressed as the mean (±SEM) of 10 animals assayed in two pools of five. Dunn's multiple comparison test p values: $^{**}p < 0.01$, $^{***}p < 0.001$, $^{****}p < 0.0001$. **D)** ICS for the percentage of $CD4^+$ IL17 secreting T cells in the lung of mice 2 weeks after the booster. For p values, we performed the Mann-Whitney *t*-test ($^{*}p < 0.05$). **E)** ICS for the percentage of $CD4^+$ $CXCR3^+KLRG1^-$ T cells in the lung of mice 2 weeks after the booster. Mann-Whitney *t*-test p values; $^{**}p < 0.01$.**F)** ICS for the percentage of $CD4^+CXCR3^-KLRG1^+$ T cells in the lungs of mice 2 weeks after the booster. Mann-Whitney *t*-test p values; ns = $p > 0.05$. **D-F)** Data are expressed as mean (±SEM), and each symbol represents an individual animal.

boost both mucosal and peribronchial immune responses against *Mtb*.

Here, we explore the efficacy of cGAMP, a STING-agonist, as an adjuvant in an intranasal vaccine that induces Th1-specific response, lung parenchyma homing T cells in vaccinated animals and provides protection against virulent *Mtb*. The H1 antigen fusion protein and NanoSTING together protected from challenge with virulent *Mtb*. Experimental vaccinations with NanoSTING adjuvant provided protection that inhibited bacterial replication in the spleen and liver for at least four weeks following the challenge. The H1 antigen protein we utilized contains two well-characterized immunodominant proteins that induce significant T cell responses: Ag85b and ESAT-6 [44,45,46]. IFNγ secreted by $CD4^+$ T cells is essential for infection control, host survival, and long-term reduction of bacterial burden [47]. IFNγ knockout mice succumb to the *Mtb* challenge, as they fail to control bacterial replication compared to control animals [48]. Data from macaques also show that $CD4^+$ T cells may contain rapid TB progression and early bacterial

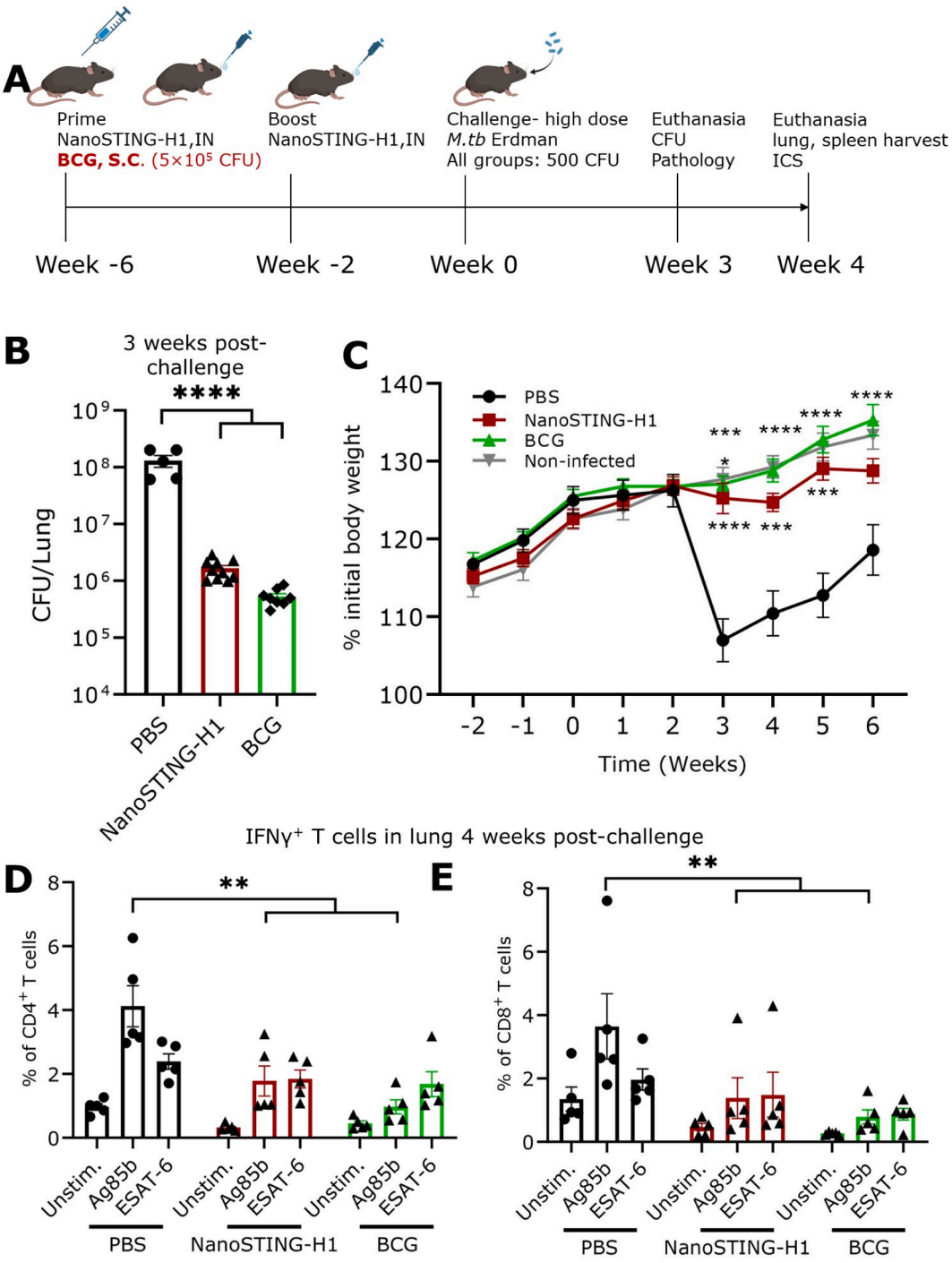

Fig. 4. Intranasal vaccination with NanoSTING-H1 provides comparable protection to BCG against aerosolized *Mtb* strain Erdman. A) We immunized 26 C57BL/6 mice intranasally that followed the prime-boost regimen used in our immunogenicity study. A group (n = 5) of mice were also immunized subcutaneously with BCG. Both groups of animals were then challenged with aerosolized *Mtb* strain Erdman. The animals were sacrificed four weeks after the challenge, and lungs and spleens were collected for CFU and flow cytometry assays. **B)** CFU counts from mice three weeks after the challenge. Mann-Whitney *t*-test p values; ****p < 0.0001. **C)** Percent bodyweight of mice compared to baseline at the indicated time intervals. Tukey's multiple comparison test p values; *p < 0.05, **p < 0.01, ***p < 0.001, ****p < 0.0001. **D, E)** ICS for percentage of Ag85B and ESAT-6 specific $CD4^+$ (D) and $CD8^+$ (E) T cells, data is presented as mean (±SEM) of five animals assayed in each group. Mann-Whitney *t*-test p values; **p < 0.01.

dissemination from the site of infection to other organs [49]. Additionally, IFNγ secreted by $CD4^+$ T cells facilitates a robust $CD8^+$ T cell response. NanoSTING, as a mucosal adjuvant, enhances IFNγ-secreting T cell response conferred by the antigens in the lung and spleen. We observe Ag85b specific CD4 + IFNγ-secreting Th1 T cells in the spleen of animals receiving NanoSTING-H1, which may explain decreased bacterial load in the spleen and liver four weeks post-challenge (**Supplementary Fig. 6**). Besides Th1 cells, the development of Th17 cells was likely related to the enhanced performance of intranasal NanoSTING-H1. While Th17 cells were shown to be dispensable for primary immunity to *Mtb* [50], they were correlated with enhanced protection against highly virulent *Mtb* strains [29]. IL-17 was also correlated with the rapid recruitment of IFNγ-producing T cells in the lung upon infection and was required for the full efficacy of a BCG

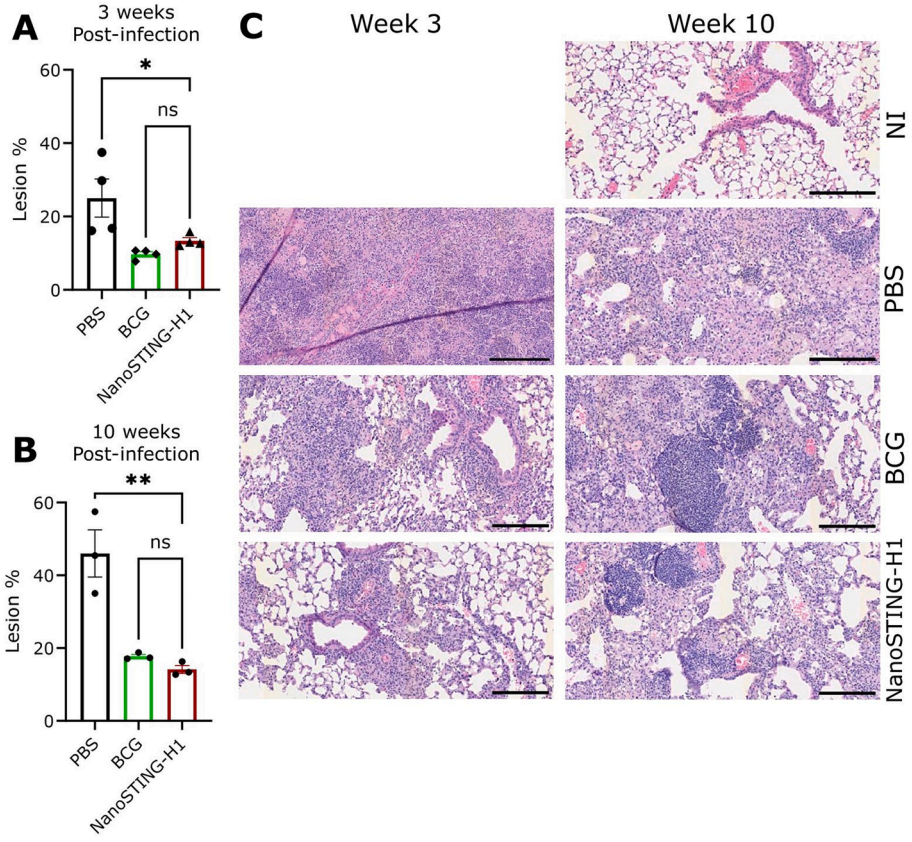

Fig. 5. Histopathological analysis of mouse lungs following *Mtb* challenge. A-B) Mean lung histopathology scores three weeks (A) and 10 weeks (B) post-infection. Mann-Whitney test p values; ns = $p > 0.05$, *$p < 0.05$. **C)** H&E staining of lung tissue from unvaccinated and non-infected (NI), unvaccinated and infected (PBS), BCG-vaccinated, and HI-vaccinated infected C57BL/6 mice at three- and 10-weeks post-challenge. Pictures are 20X enlargement showing the organized lymphocyte architecture among vaccinated (BCG and H1) mice absent in the PBS group and necrosis present in the PBS group later in disease that is prevented by vaccination. The scale bar represents 200 μm.

vaccine [51].

We observed $CD4^+$ $CXCR3^+$ $KLRG1^-$ T cells in the lungs of vaccinated animals, which are known to migrate to lung parenchyma and control bacterial infection [30]. The loss of BCG-induced protection was correlated with increased KLRG1-expressing T cells [52]. This is encouraging data, as multiple studies have suggested that $KLRG1^-$ $CD4^+$ T cells have enhanced proliferative ability and routinely replicate to replenish T cell protection at the site of infection [53,54].

The role of antibody-mediated immunity against TB remains controversial. Early studies with B cell-knockout mice indicated that antibody response against *Mtb* antigens was disposable in protection against pulmonary TB [55,56]. However, a recent clinical trial with a protein-based vaccine suggested that TB-specific antibodies may play a role in protecting high-risk BCG-primed individuals against sustained *Mtb* infection [57]. Since vaccination with NanoSTING-H1 induced modest Ag85b specific titers, further studies are warranted to test the role of these antibodies in vaccine-induced protection.

For intracellular pathogens, cyclic dinucleotides (CDN) offer much potential as a vaccine adjuvant [58]. Natural CDNs can prime innate immunity through the cGAS-STING pathway. Van Dis *et al.* have recently demonstrated the efficacy of STING-agonist cyclic dinucleotide adjuvant in a protein-based intranasal vaccine against TB [5]. Their adjuvant ML-RR-cGAMP was modified to include phosphorothioate internucleotide linkages, which protects it from hydrolysis by phosphodiesterases. However, we take advantage of nanoparticles to encapsulate and deliver cGAMP to the antigen-presenting cells, bypassing the problem of extracellular hydrolysis. The endogenous 2′-3′ cGAMP, the adjuvant in our vaccine, exhibits higher binding affinity to STING among cGAMP molecules containing other phosphodiester linkages [59]. Additionally, liposomal NanoSTING increases the residence time of H1 antigen in the nasal cavity, which may explain the need for only a single booster dose to yield BCG-comparable protection in the lung.

H1, the fusion protein used in this study, is a model antigen that has an extensive track record in subunit vaccines with or without adjuvants [46,60,61,62]. H1 antigen was designed initially as a prophylactic vaccine intended to improve the efficacy of BCG [63] but provided limited protection in the latent phase of *Mtb* infection [64]. To enhance disease outcome post-*Mtb* exposure, several therapeutic subunit vaccines have been developed, including ID93+GLA-SE [65], H56:IC31 [64], and $M72/AS01_E$ [66]. These vaccines target late antigens from *Mtb* (e.g., Rv2600c [61] and Rv1813 [67]) that are selectively expressed by the bacteria for long-term survival. It would be interesting to test the efficacy of our adjuvant formulation in a multistage vaccine by including the latency-associated antigens from *Mtb*. Thus, newer antigen strategies are needed to realize the full potential of NanoSTING as an adjuvant in a vaccine against TB.

We have demonstrated that, at least in the short term, the protection afforded by intranasal vaccination with NanoSTING-H1 is comparable to the protection afforded by vaccination with BCG. The advantage of mucosal vaccines, as we have demonstrated with respiratory viruses, is that they can prime mucosal immunity in the respiratory tract and can prevent the transmission of the pathogen by vaccinated animals [15]. In the case of TB, however, there is a lack of established animal models to study vaccine efficacy against *Mtb* transmission between animals [68]. In the future, it would be interesting to examine whether mucosal vaccines adjuvanted with NanoSTING can protect against initial infection in a transmission-permissive animal model.

This study shows that nanoparticles encapsulating 2′-3′- cGAMP are

an effective adjuvant against virulent *Mtb* infection in mice. NanoSTING is a promising candidate for developing a safe and potent subunit vaccine for immunocompromised individuals. This preliminary work warrants further investigations into vaccine formulations with NanoSTING and next-generation TB antigens for enhanced protection against TB.

CRediT authorship contribution statement

K M Samiur Rahman Sefat: Writing – review & editing, Writing – original draft, Project administration, Methodology, Formal analysis, Data curation, Conceptualization. **Monish Kumar:** Writing – original draft, Project administration, Methodology, Investigation, Formal analysis, Data curation, Conceptualization. **Stephanie Kehl:** Methodology, Formal analysis, Data curation. **Rohan Kulkarni:** Data curation. **Ankita Leekha:** Data curation. **Melisa-Martinez Paniagua:** Data curation. **David F. Ackart:** Data curation. **Nicole Jones:** Data curation. **Charles Spencer:** Formal analysis, Data curation. **Brendan K Podell:** Methodology, Formal analysis, Data curation. **Hugues Ouellet:** Supervision, Methodology, Investigation, Formal analysis, Data curation. **Navin Varadarajan:** Writing – review & editing, Writing – original draft, Supervision, Resources, Project administration, Formal analysis, Conceptualization.

Declaration of competing interest

The authors declare the following financial interests/personal relationships which may be considered as potential competing interests: Navin Varadarajan reports financial support was provided by National Institutes of Health. Navin Varadarajan reports financial support was provided by AuraVax Therapeutics. Navin Varadarajan reports a relationship with AuraVax Therapeutics and CellChorus that includes: equity or stocks.

Data availability

Data will be made available on request.

Acknowledgments

This publication was supported by the NIH (R01GM143243) and AuraVax Therapeutics.

Authorship contribution

Designed the study: SRS, MK, HO, NV. Prepared the manuscript: SRS, MK, NV. Performed experiments: SRS, MK, SK, RK, AL, MMP, NJ, CS, BP, HO. Analyzed data: SRS, MK, SK, NJ, HO. All authors edited and approved the manuscript.

Appendix A. Supplementary data

Supplementary data to this article can be found online at https://doi.org/10.1016/j.vaccine.2024.04.055.

References

[1] Young D, Dye C. The development and impact of tuberculosis vaccines. Cell Feb. 2006;124(4):683–7. https://doi.org/10.1016/j.cell.2006.02.013.
[2] Hawn TR, et al. Tuberculosis vaccines and prevention of infection. Microbiol Mol Biol Rev Dec. 2014;78(4):650–71. https://doi.org/10.1128/MMBR.00021-14.
[3] Marais BJ, et al. Interrupted BCG vaccination is a major threat to global child health. Lancet Respir Med Apr. 2016;4(4):251–3. https://doi.org/10.1016/S2213-2600(16)00099-0.
[4] Lee S, Nguyen MT. Recent advances of vaccine adjuvants for infectious diseases. Immune Network Apr. 2015;15(2):51–7. https://doi.org/10.4110/in.2015.15.2.51.
[5] Van Dis E, et al. STING-activating adjuvants Elicit a Th17 immune response and protect against mycobacterium tuberculosis infection. Cell Rep May 2018;23(5):1435–47. https://doi.org/10.1016/j.celrep.2018.04.003.
[6] Paquin-Proulx D et al. Latent Mycobacterium tuberculosis Infection Is Associated With a Higher Frequency of Mucosal-Associated Invariant T and Invariant Natural Killer T Cells. Front. Immunol, 2018; 9 Accessed: Apr. 05, 2023. [Online]. Available: https://www.frontiersin.org/articles/10.3389/fimmu.2018.01394.
[7] Macpherson AJ, McCoy KD, Johansen F-E, Brandtzaeg P. The immune geography of IgA induction and function. Mucosal Immunol Jan. 2008;1(1):11–22. https://doi.org/10.1038/mi.2007.6.
[8] Lycke N. Recent progress in mucosal vaccine development: potential and limitations. Nat Rev Immunol 2012;12(8):8. https://doi.org/10.1038/nri3251.
[9] Stylianou E, Paul MJ, Reljic R, McShane H. Mucosal delivery of tuberculosis vaccines: a review of current approaches and challenges. Expert Rev Vaccines Dec. 2019;18(12):1271–84. https://doi.org/10.1080/14760584.2019.1692657.
[10] Luo J, et al. Enhancing immune response and heterosubtypic protection ability of inactivated H7N9 vaccine by using STING agonist as a mucosal adjuvant. Front Immunol 2019. https://doi.org/10.3389/fimmu.2019.02274.
[11] Wu J, et al. Cyclic GMP-AMP is an endogenous second messenger in innate immune signaling by cytosolic DNA. Science Feb. 2013;339(6121):826–30. https://doi.org/10.1126/science.1229963.
[12] Gogoi H, Mansouri S, Jin L. The age of cyclic dinucleotide vaccine adjuvants. Vaccines (Basel) Aug. 2020;8(3):453. https://doi.org/10.3390/vaccines8030453.
[13] Ning H et al. Subunit Vaccine ESAT-6:c-di-AMP Delivered by Intranasal Route Elicits Immune Responses and Protects Against Mycobacterium tuberculosis Infection. Front. Cell. Infect. Microbiol., 2021; 11, Accessed: Apr. 05, 2023. [Online]. Available: https://www.frontiersin.org/articles/10.3389/fcimb.2021.647220.
[14] An X, et al. Single-dose intranasal vaccination elicits systemic and mucosal immunity against SARS-CoV-2. iScience Sep 2021;24(9):103037. https://doi.org/10.1016/j.isci.2021.103037.
[15] Leekha A et al. Ending transmission of SARS-CoV-2: sterilizing immunity using an intranasal subunit vaccine. bioRxiv, p. 2022.07.14.500068, Jul. 15, 2022. doi: 10.1101/2022.07.14.500068.
[16] Li L, et al. Hydrolysis of 2′3′-cGAMP by ENPP1 and design of non-hydrolyzable analogs. Nat Chem Biol Dec. 2014;10(12):1043–8. https://doi.org/10.1038/nchembio.1661.
[17] Wehbe M, et al. Nanoparticle delivery improves the pharmacokinetic properties of cyclic dinucleotide STING agonists to open a therapeutic window for intravenous administration. J Control Release Feb. 2021;330:1118–29. https://doi.org/10.1016/j.jconrel.2020.11.017.
[18] Leekha A et al. An intranasal nanoparticle STING agonist has broad protective immunity against respiratory viruses and variants. bioRxiv, p. 2022.04.18.488695, Apr. 19, 2022. doi: 10.1101/2022.04.18.488695.
[19] Maceiras AR, Silvério D, Gonçalves R, Cardoso MS, Saraiva M. Infection with hypervirulent Mycobacterium tuberculosis triggers emergency myelopoiesis but not trained immunity. Front Immunol, 2023; 14 Accessed: Mar. 04, 2024. [Online]. Available: https://www.frontiersin.org/journals/immunology/articles/10.3389/fimmu.2023.1211404.
[20] Hussein J, et al. A phase I, open-label trial on the safety and immunogenicity of the adjuvanted tuberculosis subunit vaccine H1/IC31® in people living in a TB-endemic area. Trials Jan. 2018;19(1):24. https://doi.org/10.1186/s13063-017-2354-0.
[21] Mearns H, et al. H1:IC31 vaccination is safe and induces long-lived TNF-α+IL-2+ CD4 T cell responses in M. tuberculosis infected and uninfected adolescents: a randomized trial. Vaccine Jan. 2017;35(1):132–41. https://doi.org/10.1016/j.vaccine.2016.11.023.
[22] Golovanov AP, Hautbergue GM, Wilson SA, Lian L-Y. A simple method for improving protein solubility and long-term stability. J Am Chem Soc Jul. 2004;126(29):8933–9. https://doi.org/10.1021/ja049297h.
[23] Chen L, et al. Enhanced nasal mucosal delivery and immunogenicity of anti-caries DNA vaccine through incorporation of anionic liposomes in chitosan/DNA complexes. PLoS One Aug. 2013;8(8):e71953.
[24] Thirawong N, Thongborisute J, Takeuchi H, Sriamornsak P. Improved intestinal absorption of calcitonin by mucoadhesive delivery of novel pectin–liposome nanocomplexes. J Control Release Feb. 2008;125(3):236–45. https://doi.org/10.1016/j.jconrel.2007.10.023.
[25] Wu Y, et al. Thermal-sensitive hydrogel as adjuvant-free vaccine delivery system for H5N1 intranasal immunization. Biomaterials Mar. 2012;33(7):2351–60. https://doi.org/10.1016/j.biomaterials.2011.11.068.
[26] Ramvikas M, Arumugam M, Chakrabarti SR, Jaganathan KS. Nasal Vaccine Delivery. Micro and Nanotechnology in Vaccine Development, 2017, pp. 279–301, doi: 10.1016/B978-0-323-39981-4.00015-4.
[27] Joo J, Liu X, Kotamraju VR, Ruoslahti E, Nam Y, Sailor MJ. Gated luminescence imaging of silicon nanoparticles. ACS Nano Jun. 2015;9(6):6233–41. https://doi.org/10.1021/acsnano.5b01594.
[28] Zeng G, Zhang G, Chen X. Th1 cytokines, true functional signatures for protective immunity against TB? Cell Mol Immunol Mar 2018;15(3):3. https://doi.org/10.1038/cmi.2017.113.
[29] Gopal R, et al. Unexpected role for IL-17 in protective immunity against hypervirulent mycobacterium tuberculosis HN878 infection. PLoS Pathog May 2014;10(5):e1004099.
[30] Sakai S, et al. Cutting edge: control of mycobacterium tuberculosis infection by a subset of lung parenchyma-homing CD4 T cells. J Immunol Apr. 2014;192(7):2965–9. https://doi.org/10.4049/jimmunol.1400019.
[31] Melkie ST, Arias L, Farroni C, Makek MJ, Goletti D, Vilaplana C. The role of antibodies in tuberculosis diagnosis, prophylaxis and therapy: a review from the ESGMYC study group. Eur Respiratory Rev Mar 2022;31(163). https://doi.org/10.1183/16000617.0218-2021.

[32] Jong RM, et al. Mucosal vaccination with cyclic dinucleotide adjuvants induces effective T cell homing and IL-17–dependent protection against mycobacterium tuberculosis infection. J Immunol Jan. 2022;208(2):407–19. https://doi.org/10.4049/jimmunol.2100029.
[33] Gupta A, et al. Protective efficacy of Mycobacterium indicus pranii against tuberculosis and underlying local lung immune responses in guinea pig model. Vaccine Sep. 2012;30(43):6198–209. https://doi.org/10.1016/j.vaccine.2012.07.061.
[34] "Safety, Tolerability, and Immunogenicity of the Novel Antituberculous Vaccine RUTI: Randomized, Placebo-Controlled Phase II Clinical Trial in Patients with Latent Tuberculosis Infection | PLOS ONE." Accessed: Aug. 28, 2023. [Online]. Available: https://journals.plos.org/plosone/article?id=10.1371/journal.pone.0089612.
[35] Orme IM. Induction of nonspecific acquired resistance and delayed-type hypersensitivity, but not specific acquired resistance in mice inoculated with killed mycobacterial vaccines. Infect Immun Dec. 1988;56(12):3310–2. https://doi.org/10.1128/iai.56.12.3310-3312.1988.
[36] Pal PG, Horwitz MA. Immunization with extracellular proteins of Mycobacterium tuberculosis induces cell-mediated immune responses and substantial protective immunity in a guinea pig model of pulmonary tuberculosis. Infect Immun Nov. 1992;60(11):4781–92. https://doi.org/10.1128/iai.60.11.4781-4792.1992.
[37] Andersen P. Effective vaccination of mice against Mycobacterium tuberculosis infection with a soluble mixture of secreted mycobacterial proteins. Infect Immun Jun. 1994;62(6):2536–44. https://doi.org/10.1128/iai.62.6.2536-2544.1994.
[38] Roberts AD, et al. Characteristics of protective immunity engendered by vaccination of mice with purified culture filtrate protein antigens of Mycobacterium tuberculosis. Immunology Jul. 1995;85(3):502–8.
[39] Duong VT, Skwarczynski M, Toth I. Towards the development of subunit vaccines against tuberculosis: the key role of adjuvant. Tuberculosis Mar. 2023;139:102307. https://doi.org/10.1016/j.tube.2023.102307.
[40] Day CL, et al. Induction and regulation of T-cell immunity by the novel tuberculosis vaccine M72/AS01 in South African adults. Am J Respir Crit Care Med Aug. 2013;188(4):492–502. https://doi.org/10.1164/rccm.201208-1385OC.
[41] Penn-Nicholson A, et al. Safety and immunogenicity of the novel tuberculosis vaccine ID93 + GLA-SE in BCG-vaccinated healthy adults in South Africa: a randomised, double-blind, placebo-controlled phase 1 trial. Lancet Respir Med Apr. 2018;6(4):287–98. https://doi.org/10.1016/S2213-2600(18)30077-8.
[42] Luabeya AKK, et al. First-in-human trial of the post-exposure tuberculosis vaccine H56:IC31 in Mycobacterium tuberculosis infected and non-infected healthy adults. Vaccine Aug. 2015;33(33):4130–40. https://doi.org/10.1016/j.vaccine.2015.06.051.
[43] Tkachuk AP, Gushchin VA, Potapov VD, Demidenko AV, Lunin VG, Gintsburg AL. Multi-subunit BCG booster vaccine GamTBvac: assessment of immunogenicity and protective efficacy in murine and guinea pig TB models. PLoS One Apr. 2017;12(4):e0176784.
[44] Horwitz MA, Lee BW, Dillon BJ, Harth G. Protective immunity against tuberculosis induced by vaccination with major extracellular proteins of Mycobacterium tuberculosis. Proc Natl Acad Sci Feb. 1995;92(5):1530–4. https://doi.org/10.1073/pnas.92.5.1530.
[45] Baldwin SL, Bertholet S, Reese VA, Ching LK, Reed SG, Coler RN. The importance of adjuvant formulation in the development of a tuberculosis vaccine. J Immunol Mar. 2012;188(5):2189–97. https://doi.org/10.4049/jimmunol.1102696.
[46] Olsen AW, Williams A, Okkels LM, Hatch G, Andersen P. Protective effect of a tuberculosis subunit vaccine based on a fusion of antigen 85B and ESAT-6 in the aerosol guinea pig model. Infect Immun 2004;72(10):6148–50. https://doi.org/10.1128/IAI.72.10.6148-6150.2004.
[47] Green AM, DiFazio R, Flynn JL. IFN-γ from CD4 T cells is essential for host survival and enhances CD8 T cell function during mycobacterium tuberculosis infection. J Immunol Jan. 2013;190(1):270–7. https://doi.org/10.4049/jimmunol.1200061.
[48] Flynn JL, Chan J, Triebold KJ, Dalton DK, Stewart TA, Bloom BR. An essential role for interferon γ in resistance to mycobacterium tuberculosis infection. J Exp Med 1993;178(6):2249–54. https://doi.org/10.1084/jem.178.6.2249.
[49] Yao S, Huang D, Chen CY, Halliday L, Wang RC, Chen ZW. CD4+ T cells contain early extrapulmonary tuberculosis (TB) dissemination and rapid tb progression and sustain multieffector functions of CD8+ T and CD3− lymphocytes: mechanisms of CD4+ T Cell immunity. J Immunol Mar. 2014;192(5):2120–32. https://doi.org/10.4049/jimmunol.1301373.
[50] "IL-23 Compensates for the Absence of IL-12p70 and Is Essential for the IL-17 Response during Tuberculosis but Is Dispensable for Protection and Antigen-Specific IFN-γ Responses if IL-12p70 Is Available1 | The Journal of Immunology | American Association of Immunologists." Accessed: Jul. 08, 2023. [Online]. Available: https://journals.aai.org/jimmunol/article/175/2/788/36703/IL-23-Compensates-for-the-Absence-of-IL-12p70-and.
[51] Khader SA, et al. IL-23 and IL-17 in the establishment of protective pulmonary CD4 + T cell responses after vaccination and during Mycobacterium tuberculosis challenge. Nat Immunol 2007;8(4):4. https://doi.org/10.1038/ni1449.
[52] Nandakumar S, Kannanganat S, Posey JE, Amara RR, Sable SB. Attrition of T-cell functions and simultaneous upregulation of inhibitory markers correspond with the waning of BCG-induced protection against tuberculosis in mice. PLoS One Nov. 2014;9(11):e113951.
[53] Lindenstrøm T, Knudsen NPH, Agger EM, Andersen P. Control of chronic mycobacterium tuberculosis infection by CD4 KLRG1− IL-2–secreting central memory cells. J Immunol Jun. 2013;190(12):6311–9. https://doi.org/10.4049/jimmunol.1300248.
[54] Woodworth JS, Aagaard CS, Hansen PR, Cassidy JP, Agger EM, Andersen P. Protective CD4 T cells targeting cryptic epitopes of mycobacterium tuberculosis resist infection-driven terminal differentiation. J Immunol Apr. 2014;192(7):3247–58. https://doi.org/10.4049/jimmunol.1300283.
[55] Bosio CM, Gardner D, Elkins KL. Infection of B cell-deficient mice with CDC 1551, a clinical isolate of mycobacterium tuberculosis: delay in dissemination and development of lung pathology1. J Immunol Jun. 2000;164(12):6417–25. https://doi.org/10.4049/jimmunol.164.12.6417.
[56] Vordermeier HM, Venkataprasad N, Harris DP, Ivanyi J. Increase of tuberculous infection in the organs of B cell-deficient mice. Clin Exp Immunol Nov. 1996;106(2):312. https://doi.org/10.1046/j.1365-2249.1996.d01-845.x.
[57] "Prevention of M. tuberculosis Infection with H4:IC31 Vaccine or BCG Revaccination | NEJM." Accessed: Mar. 05, 2024. [Online]. Available: https://www.nejm.org/doi/full/10.1056/NEJMoa1714021.
[58] Dubensky TW, Kanne DB, Leong ML. Rationale, progress and development of vaccines utilizing STING-activating cyclic dinucleotide adjuvants. Therapeutic Adv Vaccines Nov. 2013;1(4):131–43. https://doi.org/10.1177/2051013613501988.
[59] Shi H, Wu J, Zhang X, Sun L, Chen C, Chen ZJ. Cyclic GMP-AMP containing mixed phosphodiester linkages is an endogenous high-affinity ligand for STING. Mol Cell Jul. 2013;51(2):226–35. https://doi.org/10.1016/j.molcel.2013.05.022.
[60] Langermans JAM, et al. Protection of macaques against Mycobacterium tuberculosis infection by a subunit vaccine based on a fusion protein of antigen 85B and ESAT-6. Vaccine Apr. 2005;23(21):2740–50. https://doi.org/10.1016/j.vaccine.2004.11.051.
[61] Aagaard C, et al. A multistage tuberculosis vaccine that confers efficient protection before and after exposure. Nat Med Feb 2011;17(2):2. https://doi.org/10.1038/nm.2285.
[62] Dietrich J, Billeskov R, Doherty TM, Andersen P. Synergistic effect of bacillus calmette guerin and a tuberculosis subunit vaccine in cationic liposomes: increased immunogenicity and protection1. J Immunol Mar. 2007;178(6):3721–30. https://doi.org/10.4049/jimmunol.178.6.3721.
[63] Doherty TM, Dietrich J, Billeskov R. Tuberculosis subunit vaccines: from basic science to clinical testing. Expert Opin Biol Ther Oct. 2007;7(10):1539–49. https://doi.org/10.1517/14712598.7.10.1539.
[64] Lin PL, et al. The multistage vaccine H56 boosts the effects of BCG to protect cynomolgus macaques against active tuberculosis and reactivation of latent *Mycobacterium tuberculosis* infection. J Clin Invest Jan. 2012;122(1):303–14. https://doi.org/10.1172/JCI46252.
[65] Bertholet S et al. A Defined Tuberculosis Vaccine Candidate Boosts BCG and Protects Against Multidrug-Resistant Mycobacterium tuberculosis. Sci Transl Medi Oct. 2010; 2(53): 53ra74-53ra74, doi: 10.1126/scitranslmed.3001094.
[66] "Final Analysis of a Trial of M72/AS01E Vaccine to Prevent Tuberculosis | NEJM." Accessed: Aug. 29, 2023. [Online]. Available: https://www.nejm.org/doi/full/10.1056/NEJMoa1909953.
[67] Sherman DR, Voskuil M, Schnappinger D, Liao R, Harrell MI, Schoolnik GK. Regulation of the Mycobacterium tuberculosis hypoxic response gene encoding α-crystallin. Proc Natl Acad Sci Jun. 2001;98(13):7534–9. https://doi.org/10.1073/pnas.121172498.
[68] Ramos L, Obregon-Henao A, Henao-Tamayo M, Bowen R, Lunney JK, Gonzalez-Juarrero M. The minipig as an animal model to study *Mycobacterium tuberculosis* infection and natural transmission. Tuberculosis Sep. 2017;106:91–8. https://doi.org/10.1016/j.tube.2017.07.003.